



Magnetic order in the purely organic quasi-one-dimensional ferromagnet 2-benzimidazolyl nitronyl nitroxide

Tadashi Sugano,¹ Stephen J. Blundell,^{2,*} Tom Lancaster,² Francis L. Pratt,³ and Hatsumi Mori⁴

¹*Department of Chemistry, Meiji Gakuin University, Kamikurata, Totsuka-ku, Yokohama 244-8539, Japan*

²*Department of Physics, Clarendon Laboratory, Oxford University, Parks Road, Oxford OX1 3PU, United Kingdom*

³*ISIS Facility, STFC Rutherford Appleton Laboratory, Chilton, Oxfordshire OX11 0QX, United Kingdom*

⁴*Institute for Solid State Physics, University of Tokyo, Kashiwanoha, Kashiwa 277-8581, Japan*

(Received 13 September 2010; published 4 November 2010)

We show that the quasi-one-dimensional organic ferromagnet 2-benzimidazolyl nitronyl nitroxide (2-BIMNN) undergoes a phase transition to long-range magnetic order below $T_C=1.0(1)$ K. The intrachain exchange interactions are $J/k_B=22$ K and so the low-temperature ordering demonstrates the weakness of the interchain interactions. Our electron-spin-resonance measurements provide further evidence for the one-dimensional character of the magnetic fluctuations in 2-BIMNN and, using muon-spin rotation, we are able to characterize the broad phase transition in the material. We discuss these results in the context of other spin- $\frac{1}{2}$ quasi-one-dimensional Heisenberg ferromagnets and demonstrate that 2-BIMNN is the best realization of a one-dimensional Heisenberg ferromagnet among purely organic compounds yet discovered.

DOI: [10.1103/PhysRevB.82.180401](https://doi.org/10.1103/PhysRevB.82.180401)

PACS number(s): 75.50.Xx, 76.75.+i, 75.10.Pq

Low-dimensional magnets, in particular, one-dimensional compounds have attracted considerable attention as model quantum-mechanical systems that can be used to test theories of low-dimensional interactions.^{1,2} For example, in a one-dimensional Heisenberg magnet one may write the Hamiltonian H

$$H = -J \sum_{\langle i,j \rangle} \mathbf{S}_i \cdot \mathbf{S}_j - J' \sum_{\langle i,i' \rangle} \mathbf{S}_i \cdot \mathbf{S}_{i'}, \quad (1)$$

where the first sum double counts intrachain interactions, controlled by the intrachain exchange constant J , and the second sum double counts interactions between the chains controlled by the interchain exchange constant J' .

Organic and molecular magnets have recently become of great interest to physicists and chemists³ and can be expected to provide a wealth of opportunities for studying magnetic chains. This is because both the intrachain and interchain exchange interactions can be controlled, to some extent, using chemical modifications. Although there are many examples of spin- $\frac{1}{2}$ antiferromagnetic chains, the number of examples of spin- $\frac{1}{2}$ ferromagnetic chains is much smaller. The known examples include the copper salt tetramethylammonium copper trichloride (TMCuC) which orders at 1.2 K,^{4,5} the γ phase of para-nitrophenyl nitronyl nitroxide (p -NPNN) which orders at 0.7 K (Refs. 6–8) and the CuCl_2 -sulfoxide complexes which order below around 5 K.^{9–11} The nitronyl nitroxide route to organic magnetism is particularly attractive for synthesizing organic magnets^{12,13} since a variety of organic groups can be attached to the nitronyl nitroxide neutral radical in order to produce different crystal architectures which can favor or inhibit particular intermolecular interactions. We have focused on various substituted imidazolyl nitronyl nitroxides and identified the compound 2-benzimidazolyl nitronyl nitroxide (2-BIMNN, molecular structure shown in the inset to Fig. 3) which shows ferromagnetic interactions.¹⁴ We note that the related compound 2-imidazolyl nitronyl nitroxide (2-IMNN), which

only differs from 2-BIMNN by one benzene ring, shows antiferromagnetic and not ferromagnetic interactions,¹⁴ thus demonstrating the important role of crystal packing. These compounds can also be used in the preparation of radical ion salts.¹⁵

The neutral radical 2-BIMNN was prepared according to the procedures reported in Ref. 16. The sample was characterized by measuring magnetization isotherms up to 7 T and magnetic susceptibility χ over the temperature range from 1.8 to 300 K. As reported elsewhere (Ref. 14), susceptibility data above 70 K fit to a Curie-Weiss law with a Weiss constant $\theta=+17$ K, indicating ferromagnetic interactions. A good fit down to a few Kelvin is obtained using the one-dimensional Heisenberg ferromagnetic model (χ^{1d}) (Ref. 17) with an intrachain exchange constant $J/k_B=22$ K. Below 5 K, χ exceeds χ^{1d} , but by introducing a ferromagnetic interchain coupling constant J' , the data could be successfully fitted using the mean-field¹⁸ expression $\chi = \chi^{\text{1d}} / (1 - 2zJ'\chi^{\text{1d}}/Ng^2\mu_B^2)$ yielding $zJ'/k_B = +0.24$ K.¹⁴

Crystals suitable for x-ray diffraction studies were grown by slow evaporation of solvent. X-ray diffraction intensities were recorded on a Rigaku AFC7R automatic four-circle diffractometer with graphite monochromated Mo- K_α ($\lambda = 0.71069$ Å). Intensity data were corrected for Lorentz and polarization effects but not for absorption. The crystal structures were solved by the direct methods and the positions of H atoms were calculated. A full matrix least-squares refinement was carried out, in which positions of non-H atoms were treated with anisotropic thermal parameters and those of H atoms were treated with isotropic parameters. Our determined crystal structure is in agreement with an earlier study¹⁹ and is shown in Fig. 1. The stacking of molecules along the c direction, which provides relatively poor direct overlap between singly occupied molecular orbitals on neighboring molecules,²⁰ favors ferromagnetic chain behavior in this compound.

The quasi-one-dimensional nature of magnetic interactions is also observed in the angular dependences of the

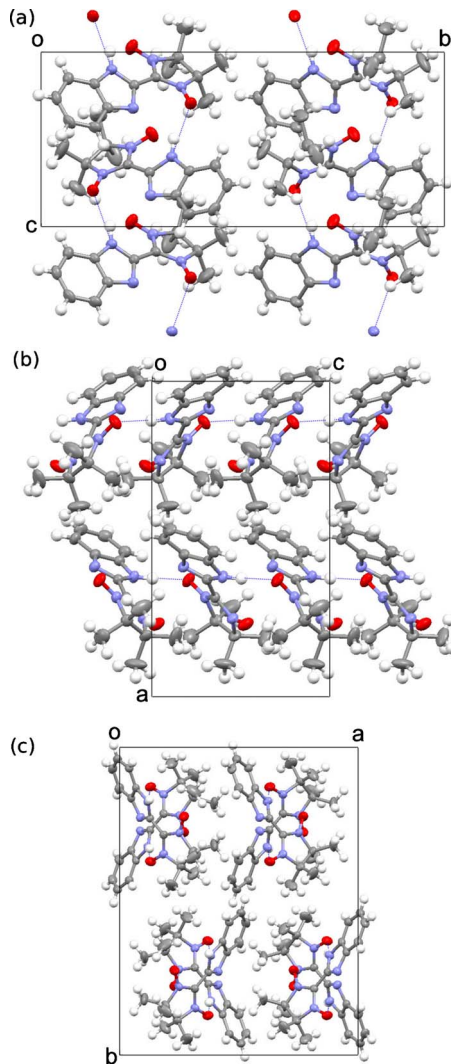


FIG. 1. (Color online) The crystal structure of 2-BIMNN projected along the (a) *a* axis, (b) *b* axis, and (c) *c* axis. The dotted lines show the dominant hydrogen bonds.

X-band electron-spin-resonance (ESR) linewidth of single-crystal samples of 2-BIMNN. The angular dependences of the peak-to-peak linewidth, B_{pp} , measured within the *ac* and *bc* planes at 292 K are plotted in Fig. 2. The angular dependences show maxima in B_{pp} whenever the applied field is parallel to the *c* axis and minima at angles of $\pm 54^\circ$ (i.e., where $3 \cos^2 \theta - 1 = 0$). This behavior is characteristic of magnetic systems where the correlation time τ_c is governed by diffusive dynamics at long times leading to $\tau_c \sim \int_0^\infty \tau^{-d/2} d\tau$, where d is the effective dimensionality of the system. This behavior was first invoked to describe the exchange narrowing observed in the antiferromagnetic chain tetramethylammonium manganese trichloride.²¹ This model of long-time diffusion, with $d=1$, leads to a prediction for the peak-to-peak ESR linewidth (neglecting any contribution from *g*-factor anisotropy) of $B_{pp} = \mathcal{A} |3 \cos^2 \theta - 1|^{4/3} + \mathcal{B}$, where \mathcal{A} and \mathcal{B} are constants, which provides a successful description of our data as shown in Fig. 2. This provides further evidence for the one-dimensional nature of the magnetic fluctuation spectrum in 2-BIMNN. Measurements at

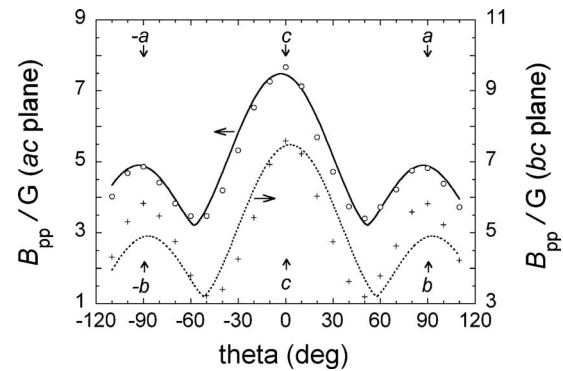


FIG. 2. Angular dependence of the peak-to-peak ESR linewidth B_{pp} within the *ac* and *bc* planes at 292 K. The angle between the one-dimensional chain axis (the *c* axis) and the applied field is θ . The open circles and crosses are experimental data and the solid and dotted lines are fitted curves (see text).

temperatures down to 100 K show no marked change in angular dependence (though B_{pp} decreases to less than one gauss) so that the data at 292 K may be considered representative of the high-temperature limit.

Muon-spin rotation²² (μ^+ SR) experiments can be particularly effective at identifying three-dimensional ordering in low-dimensional magnets since the signature of such ordering is unambiguous: a spontaneous precession of the muon-spin-polarization observed in zero-field, see, e.g., Ref. 23. This is in contrast to thermodynamic measurements, which are heavily dominated by the effect of intrachain interactions (for example, three-dimensional ordering in a very anisotropic spin chain is associated with a tiny fraction of the total entropy since, on cooling, very long correlated segments develop on individual chains in advance of the condensation of long-range order²⁴). Our μ^+ SR experiments were carried out using the low-temperature facility at the Swiss Muon Source, Paul Scherrer Institute, Switzerland. In our μ^+ SR experiment, spin-polarized positive muons (μ^+ , momentum 28 MeV/*c*) were implanted into an array of very small crystals of 2-BIMNN. The muons stop quickly (in $< 10^{-9}$ s) without significant loss of spin-polarization. The observed quantity is then the time evolution of the average muon-spin

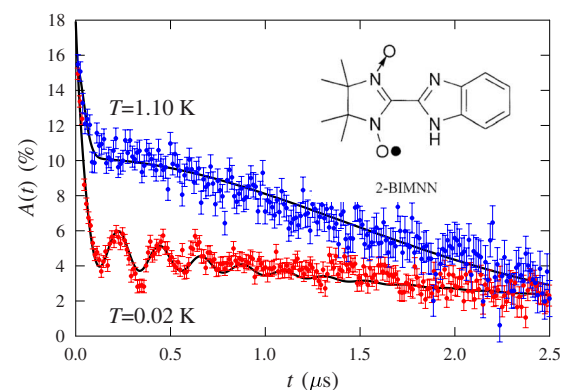


FIG. 3. (Color online) Example μ^+ SR spectra for 2-BIMNN measured above and below the magnetic transition at $T_C = 1.0(1)$ K. Inset: the molecular structure of 2-BIMNN.

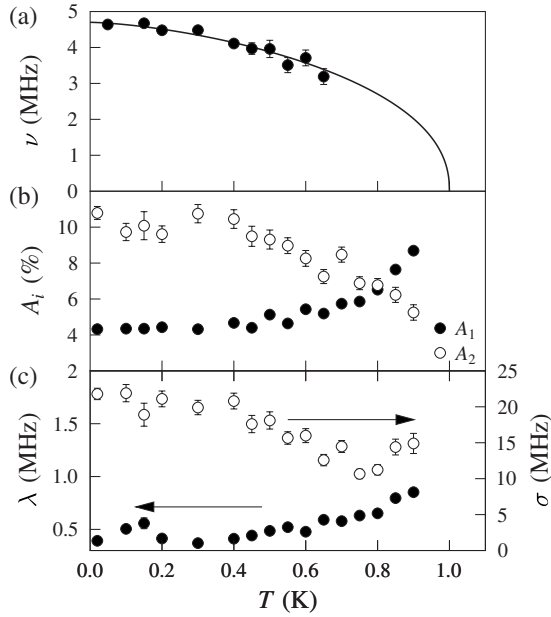


FIG. 4. Temperature evolution of the properties of the μ^+ SR spectra for $T < T_C$ from fits to Eq. (2). (a) Precession frequency (the line is a guide to the eye); (b) amplitudes of the relaxing components A_1 and A_2 ; and (c) relaxation rates λ and σ .

polarization $P_z(t)$, which can be inferred²² via the asymmetry in the angular distribution of emitted decay positrons, parameterized by an asymmetry function $A(t)$ proportional to $P_z(t)$.

Example μ^+ SR spectra are presented in Fig. 3 and show that a clear precession signal is observed at low temperature, signifying the presence of long-range magnetic order. The data are well described by the fitting function

$$A(t) = A_0 e^{-\Lambda t} \cos(2\pi\nu t + \phi) + A_1 e^{-\lambda t} + A_2 e^{-\sigma^2 t^2} + A_{\text{bg}}, \quad (2)$$

where ν is the muon precession frequency (equal to $\gamma_\mu B / 2\pi$ with B the magnetic field at the muon site and $\gamma_\mu = 2\pi \times 135.5 \text{ MHz T}^{-1}$) and A_{bg} is the background contribution from those muons that stop outside the sample. The first term, with amplitude A_0 , arises from those muons that stop in positions of quasistatic magnetic order with their spin components perpendicular to the local magnetic field at the muon site (expected to be 2/3 of the total in a polycrystalline sample). The contribution with amplitude A_1 arises from the same muon sites but with muon-spin components oriented parallel to the local magnetic field (accounting for the remaining 1/3 of the signal). The ratio was found to be $A_0/A_1 \approx 2$ as expected for a polycrystalline material. The Gaussian signal with amplitude A_2 has a large relaxation rate at the lowest measured temperatures and probably arises from a class of muon sites with a range of large local magnetic fields. The observation of this large relaxing component is common in molecular materials (see, e.g., Ref. 25), probably reflecting the variety of realized muon stopping states.

Fits to Eq. (2) reveal the temperature evolution of the precession frequency which is shown in Fig. 4(a). Above $T=0.6 \text{ K}$ the large damping of the oscillating signal causes it

TABLE I. Magnetic properties of selected one-dimensional ferromagnets. DMSO = $\text{C}_2\text{H}_6\text{SO}$, BBDDTA = benzo[1,2-*d*:4,5-*d'*]bis[1,3,2]dithiazole, TMSO = $\text{C}_4\text{H}_8\text{SO}$, and CHAC = $\text{C}_6\text{H}_{11}\text{NH}_3\text{CuCl}_3$. Other abbreviations defined in the text. β -BBDDTA·GaBr₄ contains a mixture of ferromagnetic and antiferromagnetic chains but the latter can be ignored in the low-temperature properties (Ref. 29). The interchain interactions for each compound are also ferromagnetic, except for $\text{CuCl}_2(\text{DMSO})$ and $\text{CuCl}_2(\text{TMSO})$ where they are antiferromagnetic.

| Compound | Reference | J/k_B (K) | T_C (K) | T_C/J |
|--|--------------|----------------|--------------|-----------|
| γ -NPNN | 7 | 2.15 | 0.65 | 0.30 |
| $\text{Me}_3\text{NHCuCl}_3 \cdot 2\text{H}_2\text{O}$ | 28 | 0.85 | 0.165 | 0.19 |
| $\text{CuCl}_2(\text{DMSO})$ | 9 and 10 | 45 | 4.8 | 0.11 |
| β -BBDDTA·GaBr ₄ | 29 | 4.35 | 0.4 | 0.09 |
| $\text{CuCl}_2(\text{TMSO})$ | 9 and 10 | 39 | 3 | 0.08 |
| CHAC | 30 and 31 | 45–53 | 2.18 | 0.04–0.05 |
| 2-BIMNN | This work | 22 | 1.0 | 0.045 |
| TMCuC | 4, 5, and 10 | 30, 45 | 1.24 | 0.03–0.04 |

to become unresolvable. However, the lack of any discontinuous change in either the shape of the relaxation or in the amplitudes of the components of the signal suggests that the ordering transition temperature is somewhat higher than $T=0.6 \text{ K}$. In fact, the shape of the spectra change more dramatically in the region $0.9 \leq T \leq 1.1 \text{ K}$ with the spectra measured for $T \geq 1.1 \text{ K}$ [Fig. 3] taking the form of a low-amplitude, fast, initial relaxation which dominates the signal at early times superposed on a large amplitude, slowly relaxing, Gaussian contribution. In fact, this is the typical $T > T_C$ spectrum observed in many molecular magnetic materials.^{23,26,27} The fast-relaxing component probably arises due to the existence of paramagnetic muon-radical states. The Gaussian contribution is characteristic of spin relaxation due to a random quasistatic distribution of local magnetic fields at diamagnetic muon sites (and is an approximation to the expected Kubo-Toyabe relaxation²²). In this temperature regime fluctuations of the electronic moments are motionally narrowed from the spectra, leaving only the contribution due to the magnetic fields arising from the disordered quasistatic nuclear magnetic moments surrounding the muon sites.

The $T < T_C$ temperature dependence of the amplitudes A_1 and A_2 and the relaxation rates λ and σ are shown in Fig. 4, where we see that A_1 increases with increasing temperature while A_2 falls. We also observe that λ_1 increases with increasing T while the Gaussian relaxation rate σ decreases. A very similar situation is observed in muon spectra measured in the ordered state of the quasi-one-dimensional $S=1/2$ antiferromagnets $\text{CuX}_2(\text{pyz})$ ($X=\text{Br}, \text{Cl}$)²⁶ and for $\text{Cu}(\text{HCO}_2)_2(\text{pyz})$.²⁷ The change in the components of the spectra is most noticeable above $T=0.8 \text{ K}$ making the transition region quite broad. However, by analogy with previous muon measurements on molecular magnetic systems^{26,27} (where a precession signal was observable up to T_C with similar amplitude behavior) we assign the transition temperature to be the point where the relaxation first takes on the high-temperature Gaussian form discussed above, giving us a transition temperature $T_C=1.0(1) \text{ K}$.

Our results on 2-BIMNN can be set in the context of other quasi-one-dimensional ferromagnets which have been discovered. The values of intrachain exchange constant J , three-dimensional ordering transition temperature T_c , and the ratio T_c/J are listed in Table I. This latter quantity is a measure of the one-dimensional nature of the ferromagnetism. It is readily seen that 2-BIMNN is among the most strongly one-dimensional of the ferromagnetic chains and holds the record

among purely organic magnets (the other purely organic compound in Table I, γ -NPNN, has a ratio of T_c/J a factor of six larger than that of 2-BIMNN).

Part of this work was carried out at the Swiss Muon Source, Paul Scherrer Institute, Villigen, Switzerland and we are grateful to C. Baines for technical support. This work is supported by the EPSRC, U.K.

*Corresponding author; s.blundell@physics.ox.ac.uk

- ¹L. J. de Jongh and A. R. Miedama, *Adv. Phys.* **23**, 1 (1974).
- ²I. Juhász Junger, D. Ihle, L. Bogacz, and W. Janke, *Phys. Rev. B* **77**, 174411 (2008).
- ³S. J. Blundell and F. L. Pratt, *J. Phys.: Condens. Matter* **16**, R771 (2004).
- ⁴C. P. Landee and R. D. Willett, *Phys. Rev. Lett.* **43**, 463 (1979).
- ⁵C. Dupas, J. P. Renard, J. Seiden, and A. Cheikh-Rouhou, *Phys. Rev. B* **25**, 3261 (1982).
- ⁶M. Takahashi, P. Turek, Y. Nakazawa, M. Tamura, K. Nozawa, D. Shiomi, M. Ishikawa, and M. Kinoshita, *Phys. Rev. Lett.* **67**, 746 (1991).
- ⁷Y. Nakazawa, M. Tamura, N. Shirakawa, D. Shiomi, M. Takahashi, M. Kinoshita, and M. Ishikawa, *Phys. Rev. B* **46**, 8906 (1992).
- ⁸M. Takahashi, M. Kinoshita, and M. Ishikawa, *J. Phys. Soc. Jpn.* **61**, 3745 (1992).
- ⁹D. D. Swank, C. P. Landee, and R. D. Willett, *Phys. Rev. B* **20**, 2154 (1979).
- ¹⁰R. D. Willett and C. P. Landee, *J. Appl. Phys.* **52**, 2004 (1981).
- ¹¹S. K. Satija, J. D. Axe, R. Gaura, R. Willett, and C. P. Landee, *Phys. Rev. B* **25**, 6855 (1982).
- ¹²M. Kinoshita, *Philos. Trans. R. Soc. London, Ser. A* **357**, 2855 (1999).
- ¹³M. Tamura, Y. Nakazawa, D. Shiomi, K. Nozawa, Y. Hosokoshi, M. Ishikawa, M. Takahashi, and M. Kinoshita, *Chem. Phys. Lett.* **186**, 401 (1991).
- ¹⁴T. Sugano, S. J. Blundell, W. Hayes, and P. Day, *Polyhedron* **22**, 2343 (2003).
- ¹⁵T. Sugano, S. J. Blundell, W. Hayes, and P. Day, *J. Phys. IV* **114**, 651 (2004).
- ¹⁶E. F. Ullman, J. H. Osiecki, D. G. B. Boocock, and R. Darcy, *J. Am. Chem. Soc.* **94**, 7049 (1972).
- ¹⁷G. A. Baker, Jr., G. S. Rushbrooke, and H. E. Gilbert, *Phys. Rev.* **135**, A1272 (1964).
- ¹⁸J. N. McElearney, D. B. Losee, S. Merchant, and R. L. Carlin, *Phys. Rev. B* **7**, 3314 (1973).
- ¹⁹N. Yoshioka, M. Irisawa, Y. Mochizuki, T. Kato, H. Inoue, and S. Ohba, *Chem. Lett.* **26**, 251 (1997).
- ²⁰K. Awaga, T. Sugano, and M. Kinoshita, *Chem. Phys. Lett.* **141**, 540 (1987).
- ²¹R. E. Dietz, F. R. Merritt, R. Dingle, D. Hone, B. G. Silbernagel, and P. M. Richards, *Phys. Rev. Lett.* **26**, 1186 (1971).
- ²²S. F. J. Cox, *J. Phys. C* **20**, 3187 (1987); S. J. Blundell, *Contemp. Phys.* **40**, 175 (1999); P. Dalmas de Réotier and A. Yaouanc, *J. Phys.: Condens. Matter* **9**, 9113 (1997).
- ²³T. Lancaster, S. J. Blundell, M. L. Brooks, P. J. Baker, F. L. Pratt, J. L. Manson, C. P. Landee, and C. Baines, *Phys. Rev. B* **73**, 020410(R) (2006).
- ²⁴S. J. Blundell, T. Lancaster, F. L. Pratt, P. J. Baker, M. L. Brooks, C. Baines, J. L. Manson, and C. P. Landee, *J. Phys. Chem. Solids* **68**, 2039 (2007).
- ²⁵J. L. Manson, M. M. Conner, J. A. Schlueter, T. Lancaster, S. J. Blundell, M. L. Brooks, F. Pratt, T. Papageorgiou, A. D. Bianchi, J. Wosnitza, and M. Whangbo, *Chem. Commun. (Cambridge)* **2006**, 4894.
- ²⁶T. Lancaster, S. J. Blundell, F. L. Pratt, M. L. Brooks, J. L. Manson, E. K. Brechin, C. Cadiou, D. Low, E. J. L. McInnes, and R. E. P. Winpenny, *J. Phys.: Condens. Matter* **16**, S4563 (2004).
- ²⁷T. Lancaster, S. J. Blundell, M. L. Brooks, P. J. Baker, F. L. Pratt, J. L. Manson, and C. Baines, *Phys. Rev. B* **73**, 172403 (2006).
- ²⁸H. A. Algra, L. J. de Jongh, W. J. Huiskamp, and R. L. Carlin, *Physica B* **92**, 187 (1977).
- ²⁹K. Shimizu, T. Gotohda, T. Matsushita, N. Wada, W. Fujita, K. Awaga, Y. Saiga, and D. S. Hirashima, *Phys. Rev. B* **74**, 172413 (2006).
- ³⁰R. D. Willett, C. P. Landee, R. M. Gaura, D. D. Swank, H. A. Groenendijk, and A. J. van Duynveldt, *J. Magn. Magn. Mater.* **15-18**, 1055 (1980).
- ³¹J. C. Schouten, G. J. van der Geest, W. J. M. de Jonge, and K. Kopinga, *Phys. Lett. A* **78**, 398 (1980).